# Theory of excitonic artificial atoms: InGaAs/GaAs quantum dots in strong magnetic fields

Shun-Jen Cheng,* Weidong Sheng, and Pawel Hawrylak
*Institute for Microstructural Sciences, National Research Council of Canada, Ottawa, Canada K1A 0R6*
(Received 14 July 2003; revised manuscript received 2 October 2003; published 30 December 2003)

We develop a theory of excitonic artificial atoms in strong magnetic fields. The excitonic atoms are formed by $N$ electrons and holes confined in a quantum dot. The single-particle levels are described by the Fock-Darwin spectrum in a magnetic field. The magnetic field induces crossing of energy levels and allows us to engineer degenerate shells. We apply exact diagonalization techniques to calculate the magnetic-field evolution of the ground state of the $N$-electron-hole complex and its emission spectra. We focus on degenerate shells and show that excitons condense into correlated states due to hidden symmetry. We relate the Fock-Darwin spectrum, hidden symmetries, and direct and exchange interaction among particles to the emission spectra as a function of number of electron-hole pairs (excitation power) and magnetic field.

DOI: 10.1103/PhysRevB.68.235330 PACS number(s): 73.21.La, 71.35.Ji, 78.67.Hc

## I. INTRODUCTION

With the high quality of their optical properties, self-assembled quantum dots (SAQD's) (Ref. 1) are considered attractive candidates for optoelectronic applications, including quantum-dot laser,[2–4] quantum dot infrared photodetectors,[5] single-photon devices[6–8], and gates for quantum computing.[9] SAQD's self-organize in the process of epitaxial growth of the semiconductor materials with different lattice constants (e.g., InAs/GaAs).[10,11] We focus in this work on InAs lens-shaped dots, with 10–20 nm diam and 2–5-nm height.[1,3,12,13] Since InAs as a low-band-gap material with direct gap is embedded by the high-band-gap material GaAs, not only electrons but also valence holes are confined. Under high excitation, electrons and holes localize in lens-shaped quantum dots and form strongly interacting exciton complexes with ''atomiclike'' properties.[14,15] The principle underlying the energy spectrum of excitonic artificial atoms is the existence of a hidden symmetry (HS).[14–16] The HS applies to quantum dots with well-defined shells of degenerate single-particle (SP) levels. The nature of electron and hole energy levels can be identified by the application of the magnetic field. In weak magnetic fields $B$, the shell degeneracy is lifted due to the orbital Zeeman effect, which resolves the SP states with different orbital angular momentum, and the HS is broken. The orbital Zeeman splitting has been successfully observed by previous magneto-photoluminescence experiments in various types of quantum dots.[18–22] These experiments indicated a possibility of destroying degeneracies existing at $B=0$ and creating new degeneracies at higher magnetic fields. However, to be able to observe and resolve the shell structure of the quantum dot ensemble, a high magnetic field as well as a high quality of uniformity of quantum dots are required. The required magnetic field should correspond to the cyclotron energy comparable to the energy spacing of electronic states in quantum dots. By exploiting the post-growth annealing to reduce energy-level spacing[23] and high magnetic fields up to 30 T, a successful observation of complete energy spectra of magnetoexciton complexes, including a clear observation of orbital-Zeeman splitting and magnetic field engineered degenerate shell structures, has been realized by $S$ Raymond *et al.*[24] This motivates our development of a theory of excitonic atoms in strong $B$, which will be presented in this paper.

We organize this paper as follows. In Sec. II, we introduce the single-particle spectrum. In Sec. III, we describe the Hamiltonian of many-exciton systems and the method of configuration interaction (CI) for the calculation of multiexciton states of dots. In Sec. IV, we discuss the excitonic artificial atom corresponding to magnetic-field-engineered degeneracy. Semianalytical results for the low-lying multiexciton states are discussed in detail. The numerical calculation of magnetophotoluminescence spectra is carried out. In Sec. V, magnetic-field evolution of the chemical potential of the excitonic artificial atom is calculated using exact diagonalization technique and discussed in detail. A generalization of the theory is carried out to describe the excitonic states, involving the magnetic-field-engineered degeneracy, with a higher exciton number and magnetic fields. We conclude in Sec. VI.

## II. SINGLE-PARTICLE STATES

In the effective-mass approximation, the effective confining potential of lens-shaped SAQD's can be well approximated by a two-dimensional harmonic potential,[25] $V_\beta(x,y)=\frac{1}{2}m_\beta^*\omega_\beta^2(x^2+y^2)$, where $\beta=e/h$ denotes electron/hole, and $m_\beta^*$ and $\omega_\beta$ are the effective mass and confinement frequency. The (SP) spectrum in the presence of the magnetic field normal to the dot plane $\vec{B}||\vec{z}$ can be solved exactly and expressed as a spectrum of two harmonic oscillators, the Fock-Darwin (FD) spectra,[26]

$$E_{n,m,\sigma}^{\beta}=\omega_+^{\beta}(n+1/2)+\omega_-^{\beta}(m+1/2),$$

with quantum numbers $n,m=0,1,2..$, and spin $\sigma=\pm 1/2$. Here the two frequencies are given by $\omega_+^{\beta}=\sqrt{\omega_\beta^2+(\omega_c^{\beta}/2)^2}+\omega_c^{\beta}/2\equiv\omega_H^{\beta}+\omega_c^{\beta}/2$ $(\omega_-^{\beta}=\omega_H^{\beta}-\omega_c^{\beta}/2)$ with hybridization frequency $\omega_H^{\beta}$ and cyclotron frequency $|\omega_c^{\beta}|=eB/m_\beta^*c$. The energy gap of a semiconductor is omitted here for brevity. The canonical angular momentum for an electron (hole) is given by $L_{n,m}^{e}=n-m(L_{n,m}^{h}=m-n)$. The spin-related terms, Zeeman and spin-orbit coupling, are weak and hence neglected here. This leads to doubly degenerate FD states due to spin.

 

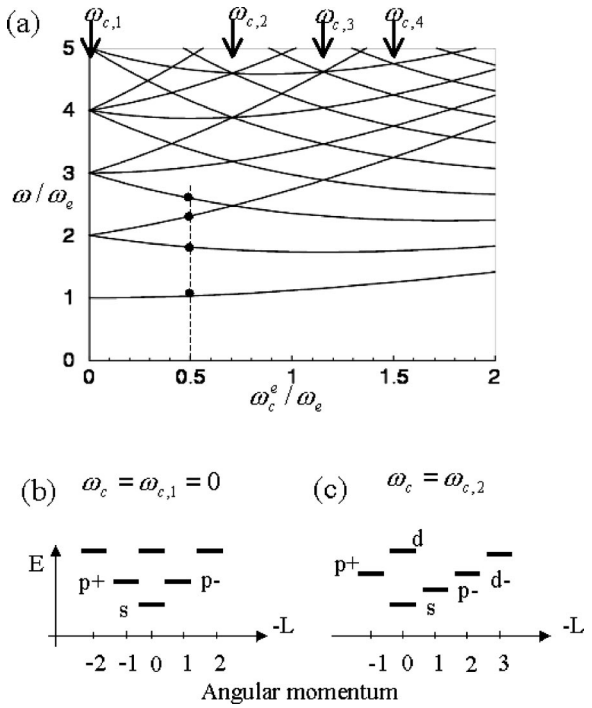


FIG. 1. (a) Fock-Darwin spectrum, in which shell structures are formed at some special magnetic fields with cyclotron frequencies, $\omega_{c,1},\omega_{c,2},..,$ (b) the three lowest shells, as $\omega_c=0$, and (c) the four lowest shells, as $\omega_c=\omega_{c,2}$, are schematically shown in the $E-L$ diagram.

At $B=0$, the states with quantum numbers satisfying $n+m=t$ and the energy $t\omega_\beta$ are degenerate and form a shell $t$ with degeneracy $g_t=t+1$ $(t=0,1,2,3..,)$. These shells are labeled $s,p,d,f,\cdots$, respectively. In finite magnetic field, the degeneracy is lifted by the orbital Zeeman effect which makes the values of $\omega_+$ and $\omega_-$ different. At special values of $B=B_s^\beta$, where $\omega_+^\beta=s\omega_-^\beta$ with $s=2,3,\ldots$, a new shell structure is formed again (see Fig. 1). This happens as cyclotron frequency has the value $\omega_c^\beta=[(s-1)/\sqrt{s}]\omega_\beta\equiv\omega_{c,s}^\beta$ (corresponding to the magnetic field $B_s^\beta\propto m_\beta^*\omega_{c,s}^\beta$). As $\omega_c=\omega_{c,s}$, the lowest shell (with $g_t>1$) consists of the state $(1,0)$ and the one of the lowest Landau level $(0,s)$.

If the effective masses and confinement frequencies of electrons and holes satisfy the relationship $m_e^*\omega_e=m_h^*\omega_h$, we have $B_s^e=B_s^h\equiv B_s$. The shell structures of electron and hole states are formed at the same magnetic field. In other words, electrons and holes possess the same FD structure, except only for different energy scale.

## III. MULTIEXCITON SYSTEM

To study excited states of the quantum dot, we replace the many-electron Hamiltonian by the electron and hole Hamiltonian. By treating electron and hole levels in the effective mass one-band approximation, we neglect the valence-band mixing effects and neglect electron-hole exchange. This allows us to focus on many-body effects and their evolution with the magnetic field. The many−electron-hole problem in this work is studied using the configuration interaction (CI) method. The many-particle configurations are built using the Fock-Darwin SP states introduced in the previous section. The interacting Hamiltonian is diagonalized exactly (exact diagonalization) in a given basis of configurations. Taking a sufficiently large number of configurations as a basis in expanding the ground and excited states of the interacting Hamiltonian, it is possible to obtain electronic states of a multiexciton system with high accuracy. In order to gain more physical insight, analytical expressions describing excitonic states in a magnetic field are derived by treating the weak Coulomb interactions as perturbation, and identifying and retaining only a few relevant configurations.

### A. The model Hamiltonian

The Hamiltonian of a multiexciton system in the language of second quantization can be written as

$$H=\sum_i E_i^e c_i^+ c_i+\sum_i E_i^h h_i^+ h_i-\sum_{ijkl} V_{ijkl}^{eh} c_i^+ h_j^+ h_k c_l + \frac{1}{2}\sum_{ijkl} V_{ijkl}^{ee} c_i^+ c_j^+ c_k c_l+\frac{1}{2}\sum_{ijkl} V_{ijkl}^{hh} h_i^+ h_j^+ h_k h_l, \quad (1)$$

where $i,j,k,l$ are the indices of FD states. The Coulomb matrix element is defined by

$$V_{ijkl}^{\beta\beta'}=\langle n_i,m_i;n_j,m_j|V_{\beta\beta'}|n_k,m_k;n_l,m_l\rangle \equiv\int\int d\vec{r_1}d\vec{r_2}\psi_i(\vec{r_1})^*\psi_j(\vec{r_2})^*[e^2/(\epsilon|\vec{r_1}-\vec{r_2}|)] \times\psi_k(\vec{r_2})\psi_l(\vec{r_1}),$$

where $\psi(\vec{r})$ is the wave function of the FD state and $\epsilon$ dielectric constant ($\epsilon=15$ is taken for InAs). The operators $c_i^+$ $(h_i^+)$ and $c_i$ $(h_i)$, respectively, create or annihilate the electron (hole) in the conduction (valence) state $|i\rangle$ with SP kinetic energy $E_i$. The matrix element of Coulomb interaction between electrons (holes) ($V^{ee}$ or $V^{hh}$) is given by[1]

$$\langle n_1'm_1';n_2'm_2'|V|n_2m_2;n_1m_1\rangle=\left(\frac{1}{l_H}\right)\frac{\delta_{R_L,R_R}(-1)^{n_2'+m_2'+n_2+m_2}}{\sqrt{n_1'!m_1'!n_1!m_1!n_2'!m_2'!n_2!m_2!}}\sum_{p_1=0}^{\min(n_1,n_1')} p_1!\binom{n_1'}{p_1}\binom{n_1}{p_1}\sum_{p_2=0}^{min(m_1,m_1')} p_2!\binom{m_1'}{p_2} \times\binom{m_1}{p_2}\sum_{p_3=0}^{\min(n_2,n_2')} p_3!\binom{n_2'}{p_3}\binom{n_2}{p_3}\sum_{p_4=0}^{\min(m_2,m_2')} p_4!\binom{m_2'}{p_4}\binom{m_2}{p_4}\left(-\frac{1}{2}\right)^p\Gamma\left(p+\frac{1}{2}\right), \quad (2)$$

where $l_H\equiv[\hbar/(2m^*\omega_H)]^{1/2}$, $R_L\equiv m_1'+m_2'-n_1'-n_2'$, $R_R\equiv m_1+m_2-n_1-n_2$, and $2p\equiv m_1+m_2+m_1'+m_2'+n_1+n_2+n_1'+n_2'-2(p_1+p_2+p_3+p_4)$. The Kronecker delta function $\delta_{R_L,R_R}$ on the right-hand-side (RHS) ensures the conservation of

total angular momentum. The strongest interaction is the direct one between $s$ states and is given by $V_0 \equiv \langle 00;00|V|00;00\rangle \propto \sqrt{\pi\omega_H}$. One can find that, in Eq. (2), the only $B$-dependent term is the form factor $1/l_H = \sqrt{2m^*\omega_H/\hbar}$. The Coulomb matrix element for finite $B$ therefore can be also expressed as $V^{ee}_{ijkl}(B) = \sqrt{(\omega^e_H/\omega_e)}V^{ee}_{ijkl}(B=0)$. The factor $\sqrt{\omega^e_H/\omega_e}(>1)$ and strength of $V^{ee}_{ijkl}(B)$ increase with increasing $B$, because the $B$ field enhances the effective confinement and reduces the average distance between particles.

The matrix element of the Coulomb interaction between an electron and a hole is given by[1]

$$\langle n'_e m'_e; n'_h m'_h|V|n_h m_h; n_e m_e\rangle = \frac{1}{l^e_H}\left(\frac{\Lambda_{eh}}{\Lambda_e}\right)^{1/2} \frac{\delta_{R_L,R_R}(\sqrt{\Lambda_{eh}/\Lambda_e})^{n'_e+m'_e+n_e+m_e}(-\sqrt{\Lambda_{eh}/\Lambda_h})^{n'_h+m'_h+n_h+m_h}}{\sqrt{n'_e!m'_e!n_e!m_e!n'_h!m'_h!n_h!m_h!}}$$
$$\times \sum_{p_1=0}^{\min(n_e,n'_e)} p_1! \binom{n'_e}{p_1}\binom{n_e}{p_1} \sum_{p_2=0}^{\min(m_e,m'_e)} p_2! \binom{m'_e}{p_2}\binom{m_e}{p_2} \sum_{p_3=0}^{\min(n_h,n'_h)} p_3! \binom{n'_h}{p_3}\binom{n_h}{p_3}$$
$$\times \sum_{p_4=0}^{\min(m_h,m'_h)} p_4! \binom{m'_h}{p_4}\binom{m_h}{p_4}\left(\frac{\Lambda_e}{\Lambda_{eh}}\right)^{p_1+p_2}\left(\frac{\Lambda_h}{\Lambda_{eh}}\right)^{p_3+p_4}\left(-\frac{1}{2}\right)^p \Gamma\left(p+\frac{1}{2}\right), \quad (3)$$

where $(\Lambda_e)^{-1} = \omega^e_c/(2\omega^e_H)$, $(\Lambda_h)^{-1} = \omega^h_c/(2\omega^h_H)$ and $(\Lambda_{eh})^{-1} \equiv \frac{1}{2}(\Lambda_h^{-1} + \Lambda_h^{-1})$. The parameters $\Lambda_{eh}$, $\Lambda_e$, and $\Lambda_h$ are introduced in Eq.(3) due to the different confinement potential for electrons and holes. In harmonic oscillators, the extention of the wave function is given by $\langle n,m|r^2_\beta|n,m\rangle \propto (1+n+m)/m_\beta\omega^\beta_H$. Accordingly, the existence of the relationship $m_e\omega^e_H = m_h\omega^h_H$ indicates that an electron and a hole in the states of QD with the same quantum number have identical envelope wave functions. This leads to $\Lambda_{eh}/\Lambda_e = \Lambda_{eh}/\Lambda_h = 1$, and makes Eq. (3) recover the form of Eq. (2).

### B. Hidden symmetries

As was shown in Refs.14–16, the similarity of $e-e$, $h-h$, and $e-h$ interactions ($\Lambda_{eh}/\Lambda_e \sim \Lambda_{eh}/\Lambda_h \sim 1$) in SAQD's leads to hidden symmetries[17] and great simplifications for interacting electron-hole complexes filling degenerate shells of a quantum dot in zero magnetic field. The HS results from the commutation relation between the Hamiltonian, Eq.(1), and the interband polarization operator $P^+ = \Sigma_i c^+_{i,\uparrow} h^+_{i,\downarrow}$ limited to shell $t$,

$$[H,P^+] \approx E^t_X P^+, \quad (4)$$

where $E^X_t = E^e_t + E^h_t - \Sigma_{jk} g_t^{-1} V^{eh}_{jjkk}$ where $E_t$, is the energy of the SP state on shell $t$. Equation (4) holds exactly for 2D electrons and holes in the lowest Landau level[17] and is well satisfied in parabolic quantum dots.[14–16] If Eq. (4) is satisfied, $N$-exciton multiplicative states $(P^+)^N|\text{vac}\rangle$ are exact eigenstates of the interacting shell Hamiltonian with energy $NE_X$. The chemical potential of the $N$-exciton system $E_X$, the energy to remove (add) an electron-hole pair to the multiplicative state, is independent of $N$ and does not depend on the filling of the shell. This could be interpreted in terms of excitons on a degenerate shell forming a noninteracting gas. In the case of an even number of excitons, one can define a singlet-singlet biexciton operator $Q^+ \equiv \frac{1}{2}\Sigma_{i,j}(c^+_{i\downarrow}c^+_{j\uparrow} + c^+_{j\downarrow}c^+_{i\uparrow})(h^+_{i\uparrow}h^+_{j\downarrow} + h^+_{j\uparrow}h^+_{i\downarrow})$. The singlet-singlet (SS) biexciton operator satisfies a commutation relation, $[H,Q^+] \approx (2E_X)Q^+$. The exact eigenstates of the multiexciton system can be constructed as $(Q^+)^{N/2}|\text{vac}\rangle$. Using hidden symmetries one can construct exact eigenstates of the electron-hole system on a degenerate shell without the need for any computation. The deviations from Eq. (4) due to different orbital character of wave functions of each shell and scattering from other shells lead to deviations of exact eigenstates from multiplicative states. These differences are shown to be small in what follows.

### C. Many-exciton states and configuration interaction

Hidden symmetries apply only to degenerate shells. The FD spectrum leads to a number of magnetic-field-engineered degeneracies. We will show that the concept of hidden symmetries can be extended to magnetic-field-engineered degeneracies. For arbitrary magnetic field no degeneracies exist and we must resort to numerical methods. To find the energy and eigenstates of the $N$-exciton system, we expand the wave function in a set of configurations, build the Hamiltonian matrix, diagonalize it, and determine the eigenstates and eigenvalues. The configurations are constructed by putting $N$ particles, according to the Pauli-exclusion principle, in $M$ ($>N$) SP states. The procedure is repeated as a function of the number of FD states and energy cutoff until convergence, for each value of the magnetic field. The number of the constructed configurations is, however, a huge number for large $M$ [for $N$ exciton, the maximum number of the configurations is $(M!/[N!(M-N)!])^2$]. The set of configurations spans our Hilbert space and determines the size of the Hamiltonian matrix needed to be solved. We can represent the many-particle states with a proper set of quantum numbers. Since the configurations with different quantum number are decoupled, we can focus each time only on a subspace spanned by the configurations with some certain quantum number to reduce numerical cost. For circular dots, total angular momentum $L$ of excitons is a good quantum number. Neglecting spin-orbit interaction, spin-flip processes are not allowed and

the $S_z$ component and the total spin S of excitons, electrons, and holes are conserved as well. The states of $N$ excitons can be represented by $|i,N,L;S^h,S_z^h;S^e,S_z^e\rangle$, where "$i$" labels states in a given Hilbert space.

Because the kinetic energy of electrons is proportional to $\omega_e$ and the Coulomb energy to $V_0 \propto \sqrt{\omega_H^e}$ ($\propto \sqrt{\omega_e}$ for $B=0$), strong confinement in dots leads to weak Coulomb scattering ($V_0/\Omega \ll 1, \Omega \equiv \omega_e + \omega_h$) among nondegenerate levels. With the small value of $V_0/\Omega$ and charge neutrality of each electron-hole pair, different configurations are coupled only through weak exchange Coulomb interactions and ground states are dominated by the configuration with lowest total SP energy. In numerical calculations, we first sort configurations according to the total SP energy and take as a basis only those with energy lower than cutoff energy $E_{\rm cut}$. The cutoff energy $E_{\rm cut}$ is increased until ground-state energy converges. Fortunately, the typical value of the ratio $V_0/\Omega$ for SAQD's is less than $\frac{1}{2}$ due to strong confinement and converged results of GS can be obtained with small value of $E_{\rm cut}$ (few $\Omega$ higher than the lowest total energy of configurations) and reasonable numerical cost.

## IV. MULTIEXCITON COMPLEXES IN MAGNETIC FIELDS

### A. Energy spectra

The main difficulty is the understanding of exciton states on degenerate shells. Let us first analyze a representative case of a doubly degenerate shell. The doubly degenerate shell at $B=0$ is the $p$ shell. In a magnetic field the degeneracy is achieved whenever the $(n=1,m=0)$ state crosses the $(m,n=0)$ states. The first magnetic-field-induced degeneracy corresponds to the magnetic-field range where $p^+$ (1,0) and $d^-$ (0,2) states are almost degenerate ($\omega_c \sim \omega_{c,2}$). The number of the excitons filling these two levels is $N=5X,.,8X$. This case corresponds to relatively low energy and low magnetic field and is most feasible in experiments. The analysis can be easily generalized to other cases with a larger number of excitons and higher magnetic fields.

#### *1. N=5X*

For $N=5X$, in the magnetic field around $B_2$ ($\omega_c^\beta \sim \omega_{c,2}^\beta = \omega_\beta/\sqrt{2}$), there are two relevant configurations, $|5X;a\rangle$ and $|5X;b\rangle$, with lowest total SP energy, as schematically shown in Fig. 2. In these configurations, the two lowest SP states (0,0)($s$ state) and (0,1) ($p^-$ state) are fully filled by four particles and the topmost particle occupies either $p^+$ or $d^-$ states. The situation is quite similar to the $3X$ for $B \sim 0$.[14] The difference is that the latter has only one filled $s$ state and the topmost occupied shell is the $p$ shell, consisting of $p^+$ and $p^-$ states.

The two lowest $5X$states correspond to electron (hole) occupying states with different angular momentum. The magnetic field induces a transition between the two states with different quantum numbers leading to a cusplike change in the ground-state energy. However, when the two states are occupied by an electron and a hole, the total angular momentum $L=0$ both for $|5X;a\rangle$ and $|5X;b\rangle$ configurations. The

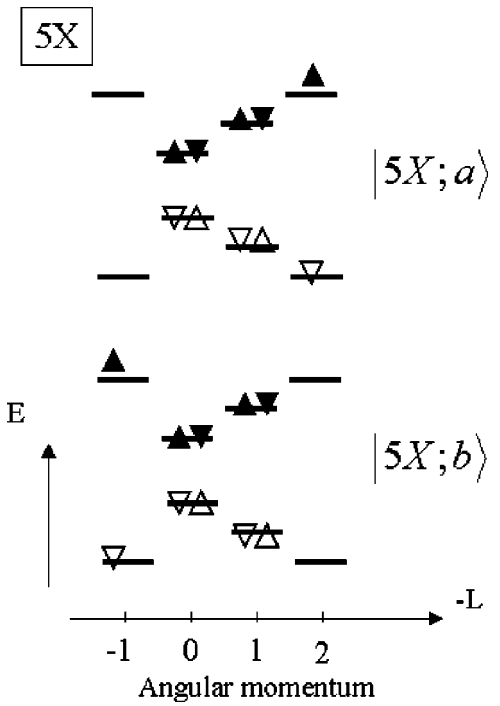


FIG. 2. The two configurations with lowest energy for $N=5X$ as $\omega_c \sim \omega_{c,2}$. The filled down (up) triangles denote electrons with spin down (up). The empty down (up) triangles denote holes with spin down (up).

two configurations are coupled and the ground state is a linear combination of states $|5X;a\rangle$ and $|5X;b\rangle$, i.e., $|\phi_{5X}\rangle \approx c_a^{5X}|5X;a\rangle + c_b^{5X}|5X;b\rangle$. Assuming that the electron and hole states with the same quantum number have the same (envelope) wave function, the Hamiltonian in the basis of $|5X;a\rangle$ and $|5X;b\rangle$ is given by

$$\hat{H}_{5X} = \begin{bmatrix} E_{4X}+E_{d^-} & -V_{eh}^{p^+d^-,x} \\ -V_{eh}^{p^+d^-,x} & E_{4X}+E_{p^+} \end{bmatrix}. \tag{5}$$

Here, $E_{4X}$ is the total energy of $N=4X$ filling the core levels. $E_{p^+} \equiv E_{1,0}^X - \Sigma_{1,0}$ is the energy of a single exciton in the $p^+$ state ($E_{1,0}^X \equiv E_{1,0}^e + E_{1,0}^h - V_{eh}^{p^+p^+,d}$), corrected by the self-energy $\Sigma_{1,0} = V_{ee}^{p^-p^+,x} + V_{ee}^{sp^+,x} + V_{hh}^{p^-p^+,x} + V_{hh}^{sp^+,x} = 2V_{ee}^{p^-p^+,x} + 2V_{ee}^{sp^+,x}$, and $E_{d^-} \equiv E_{0,2}^X - \Sigma_{0,2}$ is the corrected energy of an exciton in the $d^-$ state ($E_{0,2}^X \equiv E_{0,2}^e + E_{0,2}^h - V_{eh}^{d^-d^-,d}$ and $\Sigma_{0,2} = V_{ee}^{p^-d^-,x} + V_{ee}^{sd^-,x} + V_{hh}^{p^-d^-,x} + V_{hh}^{sd^-,x} = 2V_{ee}^{p^-d^-,x} + 2V_{ee}^{sd^-,x}$). The notation of the Coulomb interactions is intended to label corresponding orbitals and the type of interaction: $V_{eh}^{p^+p^+,d} \equiv \langle 10;10|V_{eh}|10;10\rangle$, $V_{\beta\beta}^{p^-p^+,x} \equiv \langle 10;01|V_{\beta\beta}|10;01\rangle$, $V_{\beta\beta}^{sp^+,x} \equiv \langle 10;00|V_{\beta\beta}|10;00\rangle$, $V_{eh}^{d^-d^-,d} \equiv \langle 02;02|V_{eh}|02;02\rangle$, $V_{\beta\beta}^{p^-d^-,x} \equiv \langle 02;01|V_{\beta\beta}|02;01\rangle$, $V_{\beta\beta}^{sd^-,x} \equiv \langle 02;00|V_{\beta\beta}|02;00\rangle$. Since $V_{ee}^{p^-d^-,x} = V_{hh}^{p^-d^-,x}$, we use only subscript "$ee$" to denote both for brevity. The two configurations are coupled to each other through the $e-h$ interaction, $V_{eh}^{p^+d^-,x} \equiv \langle 02;02|V_{eh}|10;10\rangle$, which is responsible for *electron-hole scattering*. The resulting two-level Hamil-

tonian Eq. (5) is similar to the effective two-level Hamiltonian describing $N=3X$ in $B\sim 0$ corresponding to one exciton in the degenerate $p$ shell.

The two eigenvalues obtained by solving Eq. (5) are $E_{5X}^{\pm}=E_{4X}+(E_{d^-}+E_{p^+})/2\mp\sqrt{(E_{d^-}-E_{p^+})^2/4+(V_{eh}^{p^+d^-,x})^2}$ ($E_{5X}^{+}=E_{5X}^{\mathrm{GS}}$ is the GS energy), and the corresponding eigenstates are given by $|\pm\rangle=1/\sqrt{(c_a^2+c_b^2)}(c_a|5X;a\rangle+c_b^{\pm}|5X;b\rangle)$ with $c_a=V^{p^+d^-,x}$ and $c_b^{\pm}=(E_{d^-}-E_{p^+})/2\pm\sqrt{(E_{d^-}-E_{p^+})^2/4+(V_{eh}^{p^+d^-,x})^2}$. When magnetic field induces degeneracy of quasiexciton energy levels $E_{d^-}=E_{p^+}$, the eigenstates are $|\pm\rangle=1/\sqrt{2}(|5X;a\rangle\pm|5X;b\rangle)$ and $E_{5X}^{\pm}=E_{4X}+(E_{d^-}+E_{p^+})/2\mp V_{eh}^{p^+d^-,x}$. The ground state $|+\rangle$ is exactly the same as that given by HS and created by $P^+$, i.e., $|+\rangle=P^+|4X\rangle$. This indicates that the HS in finite magnetic field requires the degeneracy of the states of a *quasiexciton* on the topmost shell ($E_{d^-}=E_{p^+}$ in this case), instead of that of SP states ($E_{10}=E_{02}$). Since the asymmetry of the states ($p^+$ and $d^-$) on the magnetic-field-engineered shell leads to $V^{p^+p^+,d}>V^{d^-d^-,d}$ and $\Sigma_{1,0}>\Sigma_{0,2}$, $E_{d^-}=E_{p^+}$ occurs as $\omega_c>\omega_{c,2}$, where $(E_{1,0}^e+E_{1,0}^h)-(E_{0,2}^e+E_{0,2}^h)=(V^{p^+p^+,d}+\Sigma_{1,0})-(V^{d^-d^-,d}+\Sigma_{0,2})>0$.

The numerically calculated energy spectra for $N=5X$ are shown in Fig. 4(a). For small (large) $B$, where $E_{d^-}\gg E_{p^+}$ ($E_{d^-}\ll E_{p^+}$), the ground state $|+\rangle$ is dominated by $|5X;b\rangle$ ($|5X;a\rangle$) and the GS energy $E_{5X}^{\mathrm{GS}}\approx E_{4X}+E_{p^+}$ ($E_{5X}^{\mathrm{GS}}\approx E_{4X}+E_{d^-}$). Neglecting the weak $B$ dependence of particle interactions, $E_{p^+}$ ($E_{d^-}$) has almost the same $B$ dependence as that of Fock-Darwin SP $E_{1,0}$ ($E_{0,2}$), increasing (decreasing) with $B$ in this B regime. The effect of interaction with the $N=4X$ core excitons results in the renormalized energy and magnetic field.

If $|E_{d^-}-E_{p^+}|$ is comparable to the interaction $V_{eh}^{p^+d^-,x}$, the two states are highly hybridized. Since $E_{p^+}$ and $E_{d^-}$ with the opposite $B$ dependences make a comparable contribution to $E_{5X}^{\pm}$, the $B$ dependence of $E_{5X}^{\pm}$ becomes very weak in this regime. A sharp cusp in the electron spectrum is replaced by a gradual and smooth evolution of the exciton spectrum with the magnetic field. The range of the weak $B$ dependence in magnetic field reflects the strength of the electron-hole scattering matrix element $V_{eh}^{p^+d^-,x}$.

### 2. $N=6X$

For $N=6X$, the configurations with lowest total SP energy are those with two core states filled by four excitons and two excitons in a half-filled shell consisting of orbitals $p^+-d^-$. The states of the two excitons can be classified according to total spin of electrons and of holes as singlet($S_e=0$)-singlet($S_h=0$) (SS), triplet($S_e=1$)-triplet($S_h=1$) (TT), singlet-triplet (ST), or triplet-singlet (TS). The configurations with lowest total SP energy for $6X$-SS, -TT, and -TS states are shown in Fig. 3.

The three SS configurations are given by

$$|6X;a\rangle=(c_{10\uparrow}^{+}c_{10\downarrow}^{+})(h_{10\downarrow}^{+}h_{10\uparrow}^{+})|4X\rangle, \tag{6}$$

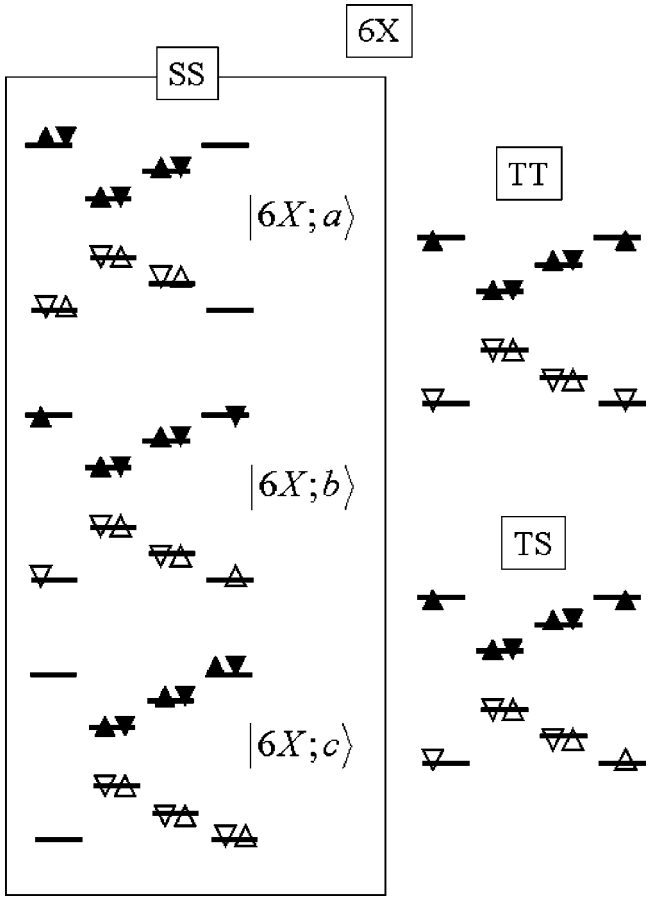


FIG. 3. The configurations with lowest energy for $N=6X$ as $\omega_c\sim\omega_{c,2}$.

$$|6X;b\rangle=\frac{1}{\sqrt{2}}(c_{10\uparrow}^{+}c_{02\downarrow}^{+}+c_{02\uparrow}^{+}c_{10\downarrow}^{+})\frac{1}{\sqrt{2}}(h_{10\downarrow}^{+}h_{02\uparrow}^{+}+h_{10\downarrow}^{+}h_{02\uparrow}^{+})|4X\rangle, \tag{7}$$

and

$$|6X;c\rangle=(c_{02\uparrow}^{+}c_{02\downarrow}^{+})(h_{02\downarrow}^{+}h_{02\uparrow}^{+})|4X\rangle. \tag{8}$$

Expanding the $6X$ states in terms of the three configurations $|6X;a\rangle,|6X;b\rangle,|6X;c\rangle$ leads to the Hamiltonian given by

$$\hat{H}_{6X}=\begin{bmatrix} E_a & -2V_{eh}^{p^+d^-,x} & 0 \\ -2V_{eh}^{p^+d^-,x} & E_b & -2V_{eh}^{p^+d^-,x} \\ 0 & -2V_{eh}^{p^+d^-,x} & E_c \end{bmatrix}, \tag{9}$$

where $E_a\equiv E_{4X}+2E_{p^+}$, $E_b\equiv E_{4X}+E_{p^+}+E_{d^-}+2V_{ee}^{p^+d^-,x}$, $E_c\equiv E_{4X}+2E_{d^-}$, and $V_{ee}^{p^+d^-,x}=V_{eh}^{p^+d^-,x}\equiv V^{p^+d^-,x}$. If $E_{d^-}=E_{p^+}\equiv E_{pd}$, the three eigenvalues are given by $E_{ss,1}=E_{4X}+2E_{pd}-2V^{p^+d^-,x}$, $E_{ss,2}=E_{4X}+2E_{pd}$, $E_{ss,3}=E_{4X}+2E_{pd}+4V^{p^+d^-,x}$, and the corresponding eigenstates are $|ss,1\rangle=1/\sqrt{3}(|6X;a\rangle+|6X;b\rangle+|6X;c\rangle)$, $|ss,2\rangle=1/\sqrt{2}(-|6X;a\rangle+|6X;c\rangle)$, $|ss,3\rangle=1/\sqrt{6}$

$(|6X;a\rangle - 2|6X;b\rangle + |6X;c\rangle)$. The results are similar to that of $4X$ in $B=0$.[14] The lowest SS state $|ss,1\rangle$ is equivalent to $Q^+|4X\rangle$.

If $|E_{d^-}-E_{p^+}|$ is nonzero but still comparable to exchange energy $V^{p^+d^-,x}$, the $6X$ states are strongly hybridized. As $E_{d^-}-E_{p^+} \gg V^{p^+d^-,x}$ ($\ll V^{p^+d^-,x}$), the eigenvalues approach the values of diagonal elements, i.e., $E_{ss,1} \approx E_{4X}+2E_{p^+}$ ($E_{ss,1} \approx E_{4X}+2E_{d^-}$), $E_{ss,2} \approx E_{4X}+E_{p^+}+E_{d^-}+2V^{p^+d^-,x}$, $E_{ss,3} \approx E_{4X}+2E_{d^-}$ ($E_{ss,3} \approx E_{4X}+2E_{p^+}$). The calculated energies of $N=6X$ SS states are denoted by solid lines in Fig. 4(b).

We now turn to the TS configuration shown in Fig. 3. The energy of the TS state is given by $E_{ts}=E_{4X}+E_{p^+}+E_{d^-}$. The energy of the TS state has a weak B dependence in the whole regime and the same value as that of the first excited SS state as $E_{d^-}=E_{p^+}$ [see Fig. 4(b)].

The configuration for the TT state is shown in Fig. 3. The energy of the TT state is given by $E_{tt}=E_{4X}+E_{p^+}+E_{d^-}-2V^{p^+d^-,x}$, having an energy lowered by $2V^{p^+d^-,x}$ from $E_{ts}$ and almost the same $B$ dependence as that of $E_{ts}$, as shown in Fig. 4(b). As $E_{d^-}=E_{p^+}$, $E_{tt}$ is equivalent to that of the SS lowest state and both are the GS. However, including the scattering to higher shells, the lowest $E_{ss}$ is lower than $E_{tt}$ and becomes the GS.[14] Comparing the lowest energies of SS, TT, and TS states, we find that the lowest singlet-singlet state is the GS of $6X$ in all of the B-regime, i.e., $E_{\rm GS}^{6X}=E_{ss,1}$.

#### *3. $N=7X$ and $N=8X$*

For $N=7X$, there are two configurations with lowest total SP energy for $S=0$, $L=0$, and $S_z^e=1/2$ (see Fig. 5). The Hamiltonian expanded in the configurations is given by

$$\hat{H}_{7X}=\begin{bmatrix} E_{4X}+2E_{d^-}+E_{p^+}-2V_{ee}^{p^+d^-,x} & -V_{eh}^{p^+d^-,x} \\ -V_{eh}^{p^+d^-,x} & E_{4X}+E_{d^-}+2E_{p^+}-2V_{ee}^{p^+d^-,x} \end{bmatrix}. \tag{10}$$

The form of Eq. (10) is quite similar to that for $5X$, except for the diagonal elements, including the total energy of three excitons occupying the $d^-$ and $p^+$ states and $4X$ GS energy $E_{4X}$. An exchange energy appears in the diagonal elements, because the two particles with the same spin occupying $d^-$ and $p^+$ states could be exchanged.

If $E_{d^-}=E_{p^+}$, the two eigenvalues are given by $E_{7X}^{\pm}=E_{4X}+3(E_{d^-}+E_{p^+})/2-2V^{p^+d^-,x} \mp V^{p^+d^-,x}$ ($E_{7X}^{+}=E_{\rm GS}^{7X}$ is the GS energy), and the corresponding eigenstates are $|\pm\rangle = 1/\sqrt{2}(|7X;a\rangle \pm |7X;b\rangle)$. The GS $|+\rangle=(P^+)^3|4X\rangle$ is consistent with the principle of HS. For $|E_{d^-}-E_{p^+}| \sim V^{p^+d^-,x}$, $E_{7X}^{\pm}$ has a smooth evolution with the B field, in analogy to the $N=5X$ system. As $E_{d^-}-E_{p^+} \gg V^{p^+d^-,x}$ ($\ll V^{p^+d^-,x}$), the eigenvalues are given by $E_{7X}^{+}=E_{\rm GS}^{7X} \approx E_{4X}+2E_{p^+}+E_{d^-}-2V^{p^+d^-,x}$ ($E_{7X}^{+}=E_{\rm GS}^{7X} \approx E_{4X}+E_{p^+}+2E_{d^-}-2V^{p^+d^-,x}$), $E_{7X}^{-} \approx E_{4X}+E_{p^+}+2E_{d^-}-2V^{p^+d^-,x}$ ($E_{7X}^{-} \approx E_{4X}+2E_{p^+}+E_{d^-}-2V^{p^+d^-,x}$).

There is only one configuration for $N=8X$, in which all states up to the $p^+-d^-$ shell are filled. The energy of the $N=8X$ system is $E_{\rm GS}^{8X}=E_{4X}+2(E_{d^-}+E_{p^+})-4V_{ee}^{p^+d^-,x}$.

### B. Magnetophotoluminescence spectra

To calculate the photoluminescence (PL) spectra, we first numerically calculate the ground and excited states for a given number of excitons $N$ using the exact diagonalization technique. We assume fast relaxation of electron-hole pairs so that the $N$-exciton system relaxes to the ground state before $e-h$ recombination takes place. The emission of a photon during recombination of one $e-h$ pair from the ground state of the $N$-exciton system involves the transition to a final state, ground and excited, of the $(N-1)$-exciton system. According to Fermi's golden rule, the intensity of PL spectra is given by

$$A(\omega,N)=\sum_f |\langle f,(N-1)|P^-|N,i\rangle|^2 \delta(E_i-E_f-\omega). \tag{11}$$

The interband polarization operator is defined by $P^- \equiv \Sigma_{i,j,\sigma} u_{ij} h_{i,\sigma} c_{j-\sigma}$ with dipole moment $u_{i,j} \equiv \langle i|\vec{E}|j\rangle$. In the dipole approximation we have $u_{i,j} \approx \delta_{i,j}$ and $P^- = \Sigma_{i,\sigma} h_{i,\sigma} c_{i-\sigma}$, which removes an electron and a hole with the *same* quantum number and *opposite* spin from the initial state. The initial state is assumed to be the ground state of the $N$ exciton system $|N,i={\rm GS}\rangle$. The transitions to all final states of the $(N-1)$-exciton system $|N-1,f\rangle$ connected by the polarization operator to the initial state are possible.

Without interactions, the energy of an emitted photon is equal to the total kinetic energy of the recombined $e-h$ pair with the same quantum number, i.e., $\hbar\omega=E_i^e+E_i^h$, and the PL has the same spectrum as that of the $e-h$ pair. In reality, the PL spectrum from an interacting $N$-exciton dot exhibits more complicated features due to interactions. Figure 6 shows the representative calculated PL spectra for initial exciton numbers $N=18$ and the magnetic field corresponding to the electron cyclotron frequency $\omega_c^e=0.5\omega_e$. The emission spectra correspond to electrons occupying successive nondegenerate states as indicated in Fig. 1(a). For a given exciton number, the spectra are composed of a number of peaks corresponding to removal of electron-hole pairs from occupied orbitals. The peaks with highest energy correspond to the transitions from the GS of the $N-$ exciton to the GS of the $(N-1)$-exciton system, and usually have high inten-

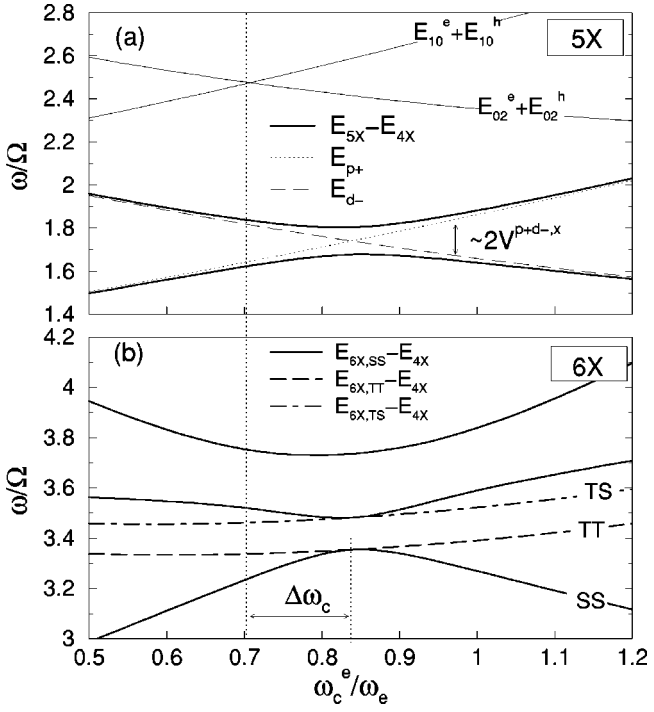


FIG. 4. (a) The calculated energies (relative to $E_{4X}$) of $5X$ states and some other relevant energies. (b) The calculated energies (relative to $E_{4X}$) of $6X$ singlet-singlet (SS), triplet-triplet (TT), and triplet-singlet (TS) states. The long vertical dotted line guides the eye to find the magnetic field ($B_2$) where $P^+$ and $d^-$ levels cross ($E_{10}=E_{02}$). HS occurs in the higher magnetic field shifted by $\Delta\omega_c$ from the magnetic field.

sity. The PL peaks at lower energies result from the transitions from the GS of the $N$ exciton to many excited states of the $(N-1)$-exciton system. They overlap with GS-to-GS transitions for lower exciton number and result in broadening of emission lines which average over the number of initial-

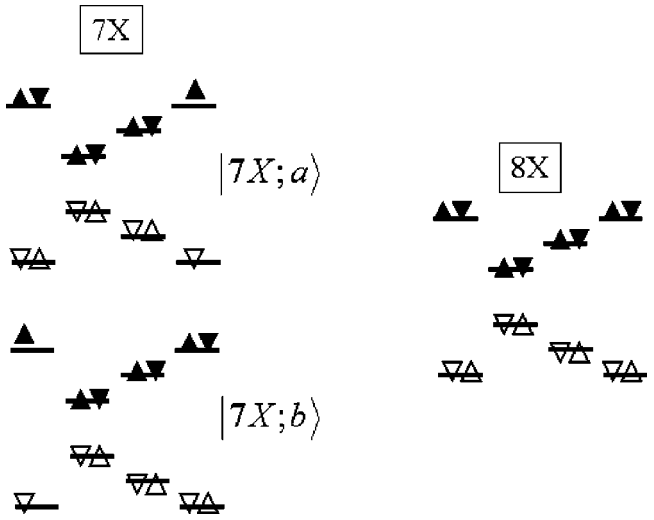


FIG. 5. The configurations with lowest energy for $N=7X$ and $8X$ as $\omega_c \sim \omega_{c,2}$.

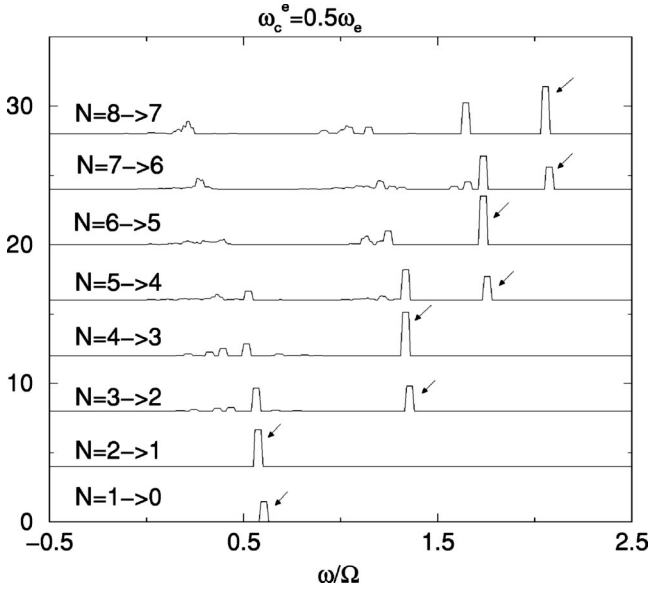


FIG. 6. Calculated PL spectra from the dots with various exciton numbers and in the magnetic field with $\omega_c^e=0.5\omega_e$. The $\omega_c^e$ and particle number are denoted in the Fock-Darwin spectrum of Fig. 1(a) by the vertical dotted line and filled circles, respectively. Arrows indicate the peaks resulting from the GS-to-GS transitions.

state excitons. Such average spectra, and their evolution with magnetic field, are well represented by considering only the main PL peaks at highest energy. Hence, the following analysis will be focused on the PL peaks corresponding to the GS-to-GS transition. The transition energy is defined as the chemical potential of the $N$-exciton system by

$$\mu_N = E_{\rm GS}^N - E_{\rm GS}^{N-1}, \tag{12}$$

where $E_{\rm GS}^N$ is the ground-state energy of the $N$-exciton system.

### C. Chemical potential

According to the $E_{\rm GS}^N$'s calculated in Sec. IV A, the chemical potential for the exciton number $N=5X,6X$ ($N=7X,8X$) in low magnetic fields where $E_{d^-}-E_{p^+} \gg V^{p^+d^-,x}$ is given by $\mu_5,\mu_6 \approx E_{p^+}$ ($\mu_7,\mu_8 \approx E_{d^-}-2V^{p^+d^-,x}$). In high magnetic fields where $E_{d^-}-E_{p^+} \ll V^{p^+d^-,x}$, we have $\mu_5,\mu_6 \approx E_{d^-}$ and $\mu_7,\mu_8 \approx E_{p^+}-2V^{p^+d^-,x}$. The renormalization $2V^{p^+d^-,x}$ for high exciton number $N=7X,8X$ is due to particle exchange. Since the Coulomb-interaction terms in $\mu_N$ are very weakly B-dependent, the B evolution of $\mu_N$ is dominated by the kinetic energies, $E_{10}$ or $E_{0,2}$, and very close to that of the SP spectrum. One hence can expect a SP-like (Fock-Darwin) spectrum of PL from the ensemble of many-exciton dots in most magnetic fields where no level crosses. In the condition of HS ($E_{p+}=E_{d-}\equiv E_{pd}$), the GS energy of the $N$-exciton system ($N=5\ldots8X$) is given by $E_{\rm GS}^N=E_{4X}+(N-4)(E_{pd}-V^{p^+d^-,x})$, and the chemical potentials given by $\mu_N=E_{pd}-V^{p^+d^-,x}$, independent of $N$.

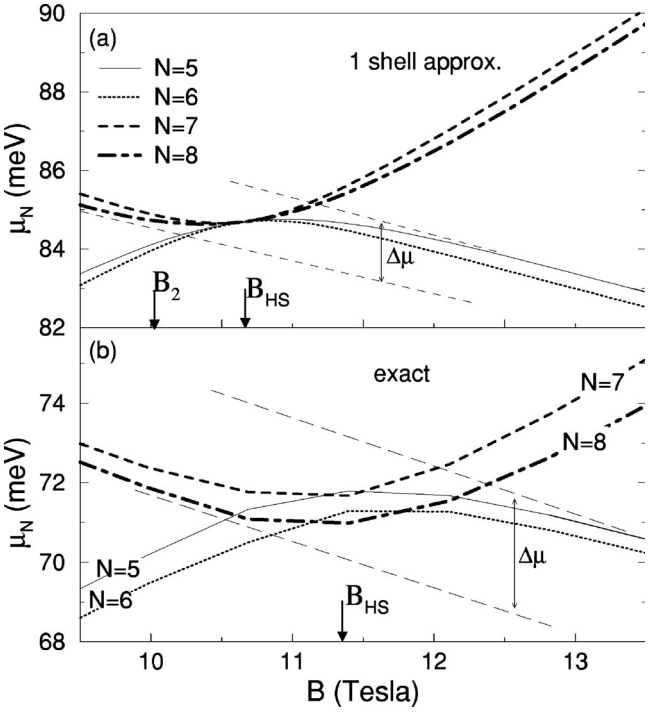


FIG. 7. The calculated chemical potential of the $N$-exciton dot for $N=5,\ldots,8X$ and $\omega_c \sim \omega_{c,2}$. The dot parameters: $\omega_e = 33\text{meV}, \omega_h = 6.6$ meV, $m_e^* = 0.05m_0$, and $m_h^* = 0.25m_0$. (a) The result calculated in the simplified model, in which only the SP $p^+$ and $d^-$ levels are considered; (b) the result calculated using the exact diagonalization technique and taking into account the seven lowest SP (doubly degenerate) states. $\Delta\mu$ denotes the offset between the two extrapolated lines and reflects the strength of exchange energy $V^{p^+d^-,x}$. $B_2$ is the magnetic field where SP states $p^+$ and $d^-$ are degenerate. $B_{\rm HS}$ is the magnetic field where hidden symmetry occurs.

Numerical calculation based on the method of CI is carried out. For simplicity, we first consider only the $p^+$ and $d^-$ SP levels in the calculation. We take the dot parameters, $\omega_e = 33$ meV, $\omega_h = 6.6$ meV, $m_e^* = 0.05m_0$, and $m_h^* = 0.25m_0$. The parameters are extracted from both PL measurement[24] on InGaAs/GaAs intermixed quantum dots and corresponding calculations using eight-band $\vec{k}\cdot\vec{p}$ theory including strain and Ga diffusion.[27,28] With those parameters, the $p^+$ and $d^-$ levels form a degenerate shell at the corresponding magnetic field of $\omega_c = \omega_{c,2}$, $B_2 = 10.1$ T [see Fig.7(a)]. This simplified model is the same as that used in Sec. IV except for the disregard of the filled core states, i.e., setting $\Sigma_{10} = \Sigma_{02} = 0$. The numerically calculated $\mu_N$'s are shown in Fig. 7(a). We see that the $\mu_N$'s for all $N$ reach their local minimum or maximum and possess the same value at $B \sim 10.6$ T$\equiv B_{\rm HS}$, where $E_{p^+} = E_{d^-}$ and hidden symmetry occurs. The renormalization of $B_{\rm HS}$ ($>B_2$) is due to the fact that $V^{p^+p^+,d} > V^{d^-d^-,d}$. The change of $\mu_N$ is insensitive to $B \sim B_{\rm HS}$, like that of $E_{\rm GS}^N$ (see discussion in Sec. IV), due to the strong hybridization of $p^+$- and $d^-$-like states. Far away from the $B_{\rm HS}$, the B evolutions of $\mu_N$'s approach that of SP energies, $E_{10}$ or $E_{02}$. The renormalization of $\mu_7$ and $\mu_8$ can be identified by extrapolating the low-field part of $\mu_7$ and $\mu_8$ into the high field and the high-field part of $\mu_5$ and $\mu_6$ into the low field (see the $\Delta\mu \sim 2V^{p^+d^-,x}$ in Fig. 7).

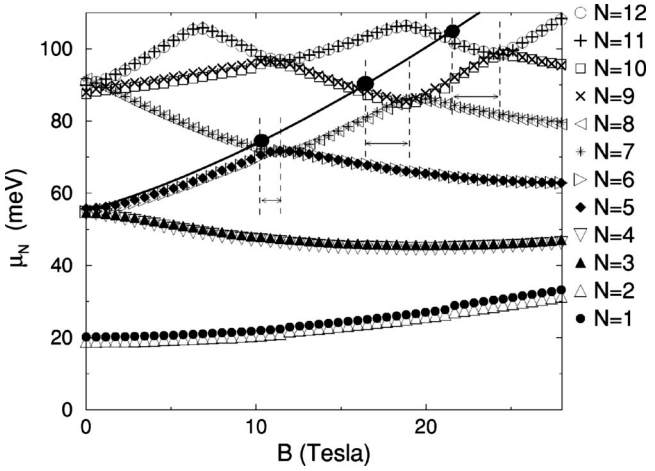


FIG. 8. The magnetospectra of chemical potentials of $N$-exciton dots for $N=1...,12X$ and the same dot parameters as those for Fig. 7, calculated using the technique of exact diagonalization. The thick solid line with the $B$ dependence of the $p^+$ SP energy ($E_{10}$) is shown for comparison with $E_{p^+}$-like chemical potentials. The filled circles on the line denote the position where the SP levels, [$p^+ = (1,0)$ and $(0,m)$ $(m=2,3,4)$], cross. Due to particle interactions the hidden symmetry, where $\mu_N$ curves stick, occurs with the renormalized fields and energies. The double-arrow lines show the renormalization of the magnetic field.

The $\mu_N$'s calculated using the exact diagonalization technique are shown in Fig. 7(b). Seven doubly degenerate low-lying SP levels are used to build up the configurations. Convergence of calculated results is achieved with a small cutoff energy of configuration, which is $1.5\times(\omega_e+\omega_h)$ higher than the lowest energy of configuration. Compared with Fig. 7(a), we find that the calculated $\mu_N$'s in Fig. 7(b) are further renormalized. This is mainly due to the finite self-energies $\Sigma_{10}$ and $\Sigma_{02}$ that result from the particle exchange involving the filled core states. And, the inequality of the two self-energies ($\Sigma_{10} > \Sigma_{02}$) shifts the $B_{\rm HS}$ further to the higher field ($\sim 11.4$ T). Besides, the $\mu_N$'s at $B \approx B_{\rm HS}$ are not any more independent of $N$ but vary slightly with $N$ due to particle scattering to the higher levels. The $\mu_N$'s for even $N$ have lower values than those for odd $N$ and the small energy difference indicates the weak biexciton binding.[13,16] As a result, the $\mu_N$ curves overlap each other in a wide range of magnetic field around $B_{\rm HS}$ (between 10.5 and 12 T).

Figure 8 shows the calculated $\mu_N$ for $N=1\cdots12X$ and $B$ up to 30 T, using the same procedure of exact diagonalization and the same dot parameters. The overlap of $\mu_N$'s curves for higher $N$ occurs again in the higher $B$ where new HS is created. The significant renormalization of $B_{\rm HS}$, indicated by double-arrow lines, can be easily indentified by comparing the $B_{\rm HS}$'s with the magnetic fields where SP levels cross. The overlap of the $\mu_N$'s curves indicates that the weakly $B$-dependent PL peaks from the ensemble of the dots with the $N$'s are superimposed in a wide range of magnetic field and a highly bright, plateaulike feature of measured magneto-PL spectrum is therefore expected in experiment.

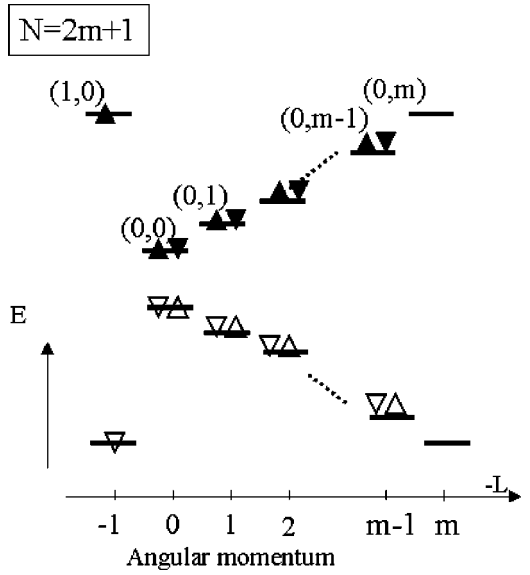


FIG. 9. One of the configurations for the exciton number $N=2m+1$ and $\omega_c \sim \omega_{c,m}$.

### D. Magnetically engineered twofold degeneracy

The above analysis can be extended to consider the generalized cases in which the topmost occupied shell consists of twofold degenerate states (1,0) and $(0,m)$, and the filled core shells are the states $(0,0),(0,1)\cdots(0,m-1)$ (the lowest Landau level), with $N=2m+1,..,2m+4$ and $\omega_c \sim \omega_{c,m}$. One representative configuration is shown in Fig. 9. The HS occurs as $E_{p^+}=E_m \equiv E_{pm}$, where $E_m$ is the energy of the quasiexciton in the $(0,m)$ states and given by $E_m=E^e_{0,m}+E^h_{0,m}-V^{mm,d}_{eh}-2\Sigma^{m-1}_{i=0}V^{mi,x}_{ee}$ ($V^{mm,d}_{eh} \equiv \langle 0m,0m|V_{eh}|0m,0m\rangle, V^{mi,x}_{ee} \equiv \langle 0m,0i|V_{ee}|0m,0i\rangle$). The energy of a quasiexciton in the $p^+$ state, as a function of the number of filled core levels $m$, is given by

$$E_{p^+}(m)=E^e_{1,0}+E^h_{1,0}-V^{p^+p^+,d}_{eh}-2\sum_{i=0}^{m-1}V^{p^+i,x}_{ee}. \quad (13)$$

One sees that, with larger $m$, $E_m$ and $E_{p^+}(m)$ gain more exchange energy. Furthermore, a higher number of core states makes the difference of the interaction parts of $E_{p^+}$ and $E_m$ larger. As a result, the HS ($E_{p^+}=E_m$) for larger $m$ occurs at the $B_{\rm HS}$ with the cyclotron frequency $\omega_c$ farther from $\omega_{c,m}$. The generalized description of GS energy for $N=2m+1,..,2m+4$ in the condition of HS is expressed as

$$E^N_{\rm GS}=E_{2mX}+(N-2m)(E_{pm}-V^{p^+m,x}), \quad (14)$$

and the chemical potential is given by

$$\mu_N=E_{pm}-V^{p^+m,x}. \quad (15)$$

As $E_m-E_{p^+}(m) \gg V^{p^+m,x}$ [$E_m-E_{p^+}(m) \ll V^{p^+m,x}$], apart from the regime of HS, the chemical potentials approach $\mu_N \approx E_{p^+}(m)$ [$\mu_N \approx E_m$] for $N=2m+1$ or $2m+2$, and $\mu_N \approx E_m-2V^{pm,x}$ ($\mu_N \approx E_{p^+}(m)-2V^{pm,x}=E_{p^+}(m+1)$) for $N=2m+3$ or $2m+4$, respectively. We find that a generalized description of the $E_{p^+}$-like chemical potential for $\omega_{c,m-1}<\omega_c<\omega_{c,m}$ and $N=2m+1,2m+2$ can be simply given by

$$\mu_N=E_{p^+}(m). \quad (16)$$

Equation (16) indicates that the renormalization of the $E_{p^+}$-like chemical potential increases with increasing number of occupied lowest Landau level and the spectra in magnetic field should show a discretelike feature. Tracing the $E_{p^+}$-like chemical potential for different $N$ and comparing that with the reference curve of SP energy of the $p^+$ state $E_{10}$ in Fig. 7, one can easily identify the effect of renormalization and the relationship to the number of occupied core states.

## V. CONCLUSION

In summary, we present a theory of exciton complexes in InGaAs/GaAs self-assembled quantum dots subject to strong magnetic fields. The energy spectra and chemical potential of magnetoexciton complexes in dots are calculated in a semianalytical manner, as well as numerically using the technique of exact diagonalization. It was found that the magnetic-field evolution of the chemical potentials of $N$-exciton interacting complexes resembles that of a single-particle (Fock-Darwin) spectrum in magnetic fields where degeneracy is lacking. However, the effect of exciton-exciton interaction becomes crucial as new degeneracies are created at special values of magnetic fields. Associated with the magnetically engineered degeneracy, the similarity of $e-e$, $h-h$, and $e-h$ interactions leads to ''hidden symmetries'' and condenses the many-exciton complexes into a coherent multiplicative state. As a result, the chemical potential of an $N$ exciton dot turns out to be insensitive to magnetic fields as well as exciton number. The theory is extended to apply to the generalized cases with magnetically engineered twofold degeneracy with higher exciton number and magnetic fields. The analytical formulas for the description of the corresponding energy spectra and chemical potentials in the condition of ''hidden symmetries'' are derived.

## VI. ACKNOWLEDGMENTS

The authors thank S. Raymond, M. Potemski, and M. Korkusinski for discussions.

*Present address: Electrophysics Department, National Chiao Tung University, Hsinchu 30050, Taiwan, Republic of China; Electronic address: sjcheng@mail.nctu.edu.tw

[1] L. Jacak, P. Hawrylak, and A. Wojs, *Quantum Dots* (Springer-Verlag, Berlin, 1998).

[2] N. Kirstaedter, N.N. Ledentsov, M. Grundmann, D. Bimberg, V.M. Ustinov, S. S. Ruvimov, M.V. Maximov, P.S. Kop'ev, Zh. I. Alferov, U. Richter, P. Werner, U. Gosele, and J. Heydenreich, Electron. Lett. **30**, 1416 (1994).

[3] S. Fafard, K. Hinzer, S. Raymond, M. Dion, J. McCaffrey, Y. Feng, and S. Charbonneau, Science **274**, 1350 (1996).

[4] H. Ishikawa, H. Shoji, Y. Nakata, K. Mukai, M. Sugawara, E. Egawa, N. Otsuka, Y. Sugiyama, T. Futatsugi, and N. Yokoyama, J. Vac. Sci. Technol. A **16**, 794 (1998).

[5] B. Aslan, H.C. Liu, P. Finnie, M. Korkusinski, S.J. Cheng, and P. Hawrylak Appl. Phys. Lett. **82**, 630 (2003), and references therein.
[6] P. Michler, A. Kiraz, C. Becher, W. V. Schoenfeld, P. M. Petroff, Lidong Zhang, E. Hu, and A. Imamoglu, Science **290**, 2282 (2000).
[7] Z. Yuan, B. E. Kardynal, R. Mark Stevenson, A. J. Shields, C. J. Lobo, K. Cooper, N. S. Beattie, D. A. Ritchie, and M. Pepper, Science **295**, 102 (2001).
[8] M. Pelton, C. Santori, J. Vuckovic, Bingyang Zhang, G. S. Solomon, J. Plant, and Y. Yamamoto, Phys. Rev. Lett. **89**, 233602 (2002).
[9] M. Bayer, P. Hawrylak, K. Hinzer, S. Fafard, M. Korkusinski, Z. R. Wasilewski, O. Stern, and A. Forchel, Science **291**, 451 (2001).
[10] P. M. Petroff and S. P. Denbaars, Superlattices Microstruct. **15**, 15 (1994).
[11] D. Bimberg, M. Grundmann, and N. N. Ledentsov, MRS Bull. **31**, (1998).
[12] J. M. Moison, F. Houzay, F. Barthe, L. Leprince, E. Andre, and O. Vatel, Appl. Phys. Lett. **64**, 196 (1994).
[13] A. Wojs, P. Hawrylak, S. Fafard, and L. Jacak, Physica E (Amsterdam) **2**, 603 (1998).
[14] Pawel Hawrylak, Phys. Rev. B **60**, 5597 (1999).
[15] M. Bayer, O. Stern, P. Hawrylak, S. Fafard, and A. Forchel, Nature (London) **405**, 923 (2000).
[16] A. Wojs and P. Hawrylak, Solid State Commun. **100**, 487 (1996).
[17] I. V. Lerner and Yu. E. Lozovik, Zh. Éksp. Teor. Fiz. **80**, 1488 (1981) [Sov. Phys. JETP **53**, 763 (1981)]; D. Paquet, T. M. Rice, and K. Ueda, Phys. Rev. B **32**, 5208 (1985); A. H. MacDonald, E. H. Rezayi, *ibid.*, **42**, 3224 (1990); Yu. A. Bychkov and E. I. Rashba, *ibid.*, **44**, 6212 (1991).
[18] A. Zrenner, L. V. Butov, M. Hagn, G. Abstreiter, G. Bohm, and G. Weimann, Phys. Rev. Lett. **72**, 3382 (1994).
[19] M. Bayer, O. Schilling, A. Forchel, T. L. Reinecke, P. A. Knipp, Ph. Pagnod-Rossiaux, and L. Goldstein, Phys. Rev. B **53**, 15810 (1996).
[20] P. D. Wang, J. L. Merz, S. Fafard, R. Leon, D. Leonard, G. Medeiros-Ribeiro, M. Oestreich, P. M. Petroff, K. Uchida, N. Miura, H. Akiyama, and H. Sakaki, Phys. Rev. B **53**, 16458 (1996).
[21] R. Rinaldi, P. V. Giugno, R. Cingolani, H. Lipsanen, M. Sopanen, J. Tulkki, and J. Ahopelto, Phys. Rev. Lett. **77**, 342 (1996).
[22] S. Raymond, P. Hawrylak, C. Gould, P. Zawadzki, A. Sachrajda, S. Charbonneau, S. Fafard, D. Leonard, P. M. Petroff, and J. L. Merz, Solid State Commun. **101**, 883 (1997).
[23] S. Fafard and C. Ni. Allen Appl. Phys. Lett. **75**, 2374 (1999).
[24] S. Raymond, S. Studenikin, A. Sachrajda, Z. Wasilewski, S.J. Cheng, W. Sheng, P. Hawrylak, A. Babinski, M. Potemski, G. Ortner, and M. Bayer (unpublished).
[25] P. Hawrylak, G. A. Narvaez, M. Bayer, and A. Forchel Phys. Rev. Lett. **85**, 389 (2000).
[26] V. Fock, Z. Phys. **47**, 446 (1928); C. G. Darwin, Proc. Cambridge Philos. Soc. **27**, 86 (1930).
[27] W. Sheng and J.-P. Leburton, Phys. Rev. B **67**, 125308 (2003).
[28] W. Sheng, S.J. Cheng, and P. Hawrylak (unpublished).